Carboxylated Nanocellulose Superabsorbent: Biodegradation and Soil Water Retention Properties

Ruth M. Barajas
Monash University
Vanessa Wong
Monash University
Karen Little
Monash University
Antonio F. Patti
Monash University
Gil Garnier (gil.garnier@monash.edu)
Monash University https://orcid.org/0000-0003-3512-0056

Research Article

Keywords: Carboxylated nanocellulose, TEMPO, soil water, biodegradation, agriculture.

Posted Date: May 10th, 2021

DOI: https://doi.org/10.21203/rs.3.rs-474606/v1

Carboxylated nanocellulose superabsorbent: biodegradation and soil water retention properties

Ruth M. Barajas-Ledesma[a], Vanessa Wong[c], Karen Little[b], Antonio Patti[b*] and Gil Garnier[a*]

[a]*Bioresource Processing Research Institute of Australia (BioPRIA) and Department of Chemical Engineering, Monash University, Clayton, VIC 3800, Australia*

[b]*School of Chemistry, Monash University, Clayton, VIC 3800, Australia*

[c]*School of Earth, Atmosphere & Environment, Monash University, Clayton, VIC 3800, Australia*

*For correspondence: Gil.Garnier@Monash.edu and Antonio.Patti@Monash.edu

Keywords: *Carboxylated nanocellulose, TEMPO, soil water, biodegradation, agriculture.*

Acknowledgements. Many thanks to the Australian Research Council (ARC), Australian paper, Circa, Norske Skog, Orora, Visy and the Government of Tasmania, for financial support through the Industry Transformation Research Hub Processing Advance Lignocellulosics (PALS) grant IH130100016.

ABSTRACT

Carboxylated nanocellulose superabsorbent polymers (SAP) can be used to increase soil water retention in agriculture. The benefits investigated are influenced by the superabsorbent structure, composition and application rate.

In this study, TEMPO (2,2,6,6-tetramethylpiperidine-1-oxyl)-oxidised nanocellulose superabsorbents were prepared using three different drying techniques: freeze-dried, and oven-dried at low and high temperatures. The swelling capacity in soil water extracts was measured and compared to deionised water. Soil was amended with different application rates of these superabsorbents to evaluate the effects on water retention, microbial community and their biodegradation.

The absorption performance of nanocellulose superabsorbents is affected by the concentration and type of salts in the soil water extracts. Oven-dried at 50 °C SAP presents the highest ionic sensitivity attributed to its large number of accessible carboxylate groups. The water retention of the soil treatments increases with increasing application rate. Soil treated with the freeze-dried superabsorbent shows the highest water retention, whereas those amended with the 50°C oven-dried SAP remain moist the longest. The biodegradation rate of these materials depends on the application rate and nutrient availability. Carboxylated nanocellulose superabsorbents emerge as high-performance biodegradable materials for agricultural use, able to replace the current non-biodegradable petrochemical-based superabsorbents.

1.0 INTRODUCTION

Water is critical for agricultural production and food security. Irrigated agriculture uses about 70% of the water available for human consumption worldwide and accounts for 59% of the total fresh water in Australia (Organisation for Economic Co-operation and Development; Department of Agriculture 2020). Water availability has been impacted by climate change, drought and water shortage; its decrease has affected world agricultural development in recent years. According to Müller C. (2010), agricultural yields will decline between 2 – 15% over the next 30 years due to climate change. Hence, the efficient use of water resources is crucial for the long-term sustainability of the agricultural industry.

One strategy to optimise water retention in soils and hence making it more available to crops, is the use of superabsorbent polymers (SAPs) (Zohuriaan-Mehr et al. 2008). SAPs are three-dimensional (3D) networks of linear or branched hydrophilic polymers physically or chemically cross-linked (Guilherme et al. 2015). SAPs can absorb and hold water at hundreds of times their own weight and remain stable in their swollen state (Ahmed 2015; Ghorbani et al. 2019; Shen et al. 2016; Gross JR 1990). They have been extensively used in many applications including biomedicine (Curvello et al. 2019), food and beverages (Shewan and Stokes 2013), personal care and hygiene products (Bashari et al. 2018). In the agricultural and horticultural industries, SAPs have a range of applications which includes seed coatings, seed additives and root dips (Zohuriaan-Mehr et al. 2010). The use of SAPs in soil has improved water availability for plants (Montesano et al. 2015). SAPs have also contributed to water retention in different types of soil, significantly reducing the irrigation water consumption (Abrisham et al. 2018). SAPs also serve as soil conditioners and nutrient carriers (Guilherme et al. 2015), thereby improving soil properties and increasing crop yield (Zohuriaan-Mehr, Kabiri, and Kourosh. 2008; Guilherme et al. 2015; Reddy Kathi S. 2019).

Most of the commercially available SAPs in agriculture are petrochemical-based and made of polyacrylate (PA) or polyacrylamide (PAM). Such PA/PAM SAPs degrade very slowly into by-products increasingly raising health concerns including the formation of

68 microplastic particles which can be harmful to soil biota (Steinmetz et al. 2016; Horton et
69 al. 2017; Ramos et al. 2015). These environmental issues have led to the development of
70 superabsorbents from natural polymers, especially those made of polysaccharides such as
71 starch (Chen et al. 2004) or pectin (Guilherme et al. 2010). Most of these are produced as
72 composites in combination with synthetic polymers which decrease their biodegradability
73 and can significantly alter soil pH (Azeem et al. 2014).
74 Some of the major limitations of naturally derived SAPs are their low mechanical
75 resistance, high-cost, restricted longevity in soils and also low-absorption capacity
76 (Guilherme et al. 2015; Zohuriaan-Mehr et al. 2010). Cellulose, and especially
77 nanocellulose, has the potential to overcome these limitations because of its availability,
78 low-cost, biodegradability, hydrophilicity and high surface area (Varanasi et al. 2013;
79 Guilherme et al. 2015). Nanocellulose refers to the individual cellulose chains, also called
80 elementary fibrils, which have a diameter of 3 – 4 nm and a length > 1 – 2 μm (Lavoine
81 and Bergström 2017). Its low-density, high-strength, flexibility and tunable surface
82 chemistry make nanocellulose attractive as a material for superabsorbents.
83 Nanocellulose-based SAPs can be produced from TEMPO-mediated oxidation of
84 cellulose, currently considered as one of the most effective methods (Mendoza et al. 2019;
85 Li et al. 2013; Kabir et al. 2018). This process selectively converts the primary alcohols
86 (C6) into carboxylate groups. This surface modification provides the necessary electrostatic
87 repulsion which produces nanoscale fibres upon mechanical fibrillation (Isogai et al. 2011).
88 Recent studies have shown that the resulting material can be dried either by freeze-drying
89 or evaporative-drying to create a highly porous superabsorbent consisting of an
90 entanglement of cellulose nanofibres (CNF) of high surface area (Barajas-Ledesma et al.
91 2020). Despite these advantages, few nanocellulose-based superabsorbents have been
92 developed for application in agriculture. Though several studies have investigated
93 cellulose-based superabsorbents, most of them are crosslinked with acrylamide or acrylic
94 acid (Li and Chen 2020), reducing their biodegradability and sustainability. Only a few
95 studies have analysed nanocellulose-based superabsorbents for agriculture. For example,

Zhang et al. (2017) found that chemically cross-linked nanocellulose superabsorbent can be beneficial for seed germination. These superabsorbents can be applied as soilless culture mediums for plant growth. Mendoza et al. (2019) reported that the absorption capacity of carboxylated nanocellulose superabsorbents is dictated by the charge density and fibre content. Zhou et al. (2013) stated that CMC–acrylamide based superabsorbents containing carboxylated CNF have a water absorption capacity higher than CNF-free superabsorbent. Yet, none of these studies has evaluated the ability of nanocellulose-based superabsorbents as a water retention agent in a real soil environment nor their biodegradability under realistic conditions.

While some studies have evaluated the synthesis and formulation of nanocellulose-based superabsorbents (Li and Chen 2020; Liliana Serna and Guancha-Chalapud 2017; Mondal 2019), none has systematically compared the effect of application rate on soil water retention properties nor related those to soil microbial activity. These steps are crucial for any agriculture use, potentially compromising food security, environment and human health. The effect of a novel generation of nanocellulose superabsorbent produced from different drying methods on the superabsorbent longevity needs to be quantified.

In this study, carboxylated nanocellulose superabsorbents were prepared via TEMPO oxidation followed by high-pressure homogenization. This standard carboxylated nanocellulose was dried using three different drying techniques: freeze-drying or oven-drying at high and low temperatures. The water retention of the soil treated with these superabsorbents was quantified for agricultural use at three different application rates. Our objective is to analyse the effect of nanocellulose-based superabsorbents on microbial activity and establish a relationship with its biodegradation. This is to enable nanocellulose superabsorbent as a new class of performance, cheap and sustainable hydro-retentor for agriculture use.

2.0 MATERIALS AND METHODS

2.1 Materials

Bleached Eucalyptus Kraft (BEK) pulp was provided by Australian Paper, Maryvale, Australia. Sodium bromide (NaBr) and 2,2,6,6-Tetramethylpiperidine-1-oxyl (TEMPO) were purchased from Sigma-Aldrich. Hydrochloric acid (HCl) and sodium hydroxide (NaOH) were diluted for solutions as required and purchased from ACL Laboratories and Merck, respectively. 12% w/v sodium hypochlorite (NaClO) was purchased from Thermo Fisher Scientific and used as received. Urea, super phosphate and sulphate of potash were purchased from Richgro (Jandakot, Australia).

Soil was collected from a wheat growing property located in Ouyen, north-west Victoria (34°58'0.16"S; 142°20'45.85"E) (alkaline Calcarosol (Isbell 2016)), Soil was collected at a depth of 20-40 cm, air-dried and sieved to <2 mm. The soil was then characterised for a range of key physicochemical properties including pH, electrical conductivity and available and exchangeable cations (Table 1). Analysis was conducted by Environmental Analysis Laboratories, at Southern Cross University (Environmental Analysis Laboratory 2020), using Rayment and Lyons (Rayment 2011) standard methods.

Table 1. Characteristics of the calcarosol soil selected for the experiments.

Parameter	Calcarosol
Electrical conductivity (dS/m)[a]	0.022
pH ($CaCl_2$)	6.80
Nitrate (mg/Kg)	2.2
Ammonium (mg/Kg)	1.5
Total Carbon (%)	0.12
Total Nitrogen (%)	0.03
Organic Matter (%)	0.20
Na^+ (mg/Kg)	14
Ca^{2+} (mg/Kg)	521
Mg^{2+} (mg/Kg)	139

K^+ (mg/Kg)	156
Phosphorus (mg/Kg)	22
Effective Cation Exchange Capacity ($cmol^+$/Kg)	4.21

[a]Electrical conductivity measured in a 1:5 soil:water extract.

2.2 Superabsorbent preparation

Nanocellulose superabsorbent was prepared following the TEMPO-mediated oxidation process developed by Isogai, Saito , and Fukuzumi (2011) to achieve a carboxylate content of 1.4 mmol/g. In brief, 25 g (dry weight) of BEK pulp was suspended in 2500 mL of water containing 0.4 g and 2.5 g of dissolved TEMPO and NaBr, respectively. To achieve a carboxylate content of 1.4 mmol/g of dry fibre, 100 mL of 12% w/v NaClO were initially adjusted to pH 10 through the addition of 36% w/v HCl. The oxidation process started by adding the 100 mL of NaClO (6.6 mmol NaClO/g cellulose) drop-wise to the suspension under constant stirring. The pH of the reaction was kept at 10 via addition of 0.5M NaOH. The reaction was maintained for 3 h or until no decrease in pH was observed. The oxidised fibres were washed with deionised water, filtrated and stored refrigerated at 4 °C.

The TEMPO-oxidised pulp was dispersed in deionised water to prepare a solution of 0.5% w/v which was further fibrillated using a high-pressure homogeniser (GEA Niro Soavi Homogeniser Panda) at 1000 bar and two passes. To produce the superabsorbent materials, the resulting product from homogenisation was either freeze-dried or oven-dried. Freeze-dried superabsorbent was accomplished by freezing the nanocellulose for at least 12 h at -80°C followed by freeze-drying (Christ Alpha 2-4 LD Plus) for 2 days. Oven-dried superabsorbent was prepared by drying the nanocellulose in an oven (Thermoline BTC-9090) at either 50 °C or 105 °C until no mass loss was observed.

2.3 Soil water retention studies

i) Soil water holding capacity. The soil water holding capacity (WHC) or field capacity was determined gravimetrically by adding an excess of water to 100 g of soil into a Buchner funnel with a filter paper placed at the bottom. Water was then allowed to drain and the

saturated soil was left covered at room temperature for 48 h. After this period, the saturated soil was weighed and oven dried. The WHC was calculated as follows:

$$\mathrm{WHC} = \mathrm{m_w} - \mathrm{m_d} \quad (1)$$

Where m_w refers to the weight of the saturated soil and m_d is the mass of the dried soil. The units of WHC are in g water/100 g of soil.

ii) Water retention tests. Soils were subjected to two experiments to test the effect of freeze-dried or oven-dried superabsorbent prepared at 50 °C or 105 °C. For both studies, polypropylene containers (120 mL) were drilled with four holes of 4 mm diameter and a filter paper was placed at the bottom of each. Each experiment was then prepared as follows: superabsorbent was added to the soil at rates of 0.2, 0.5 and 1 wt% to prepare a total of 50 g of soil treatment (Table 2). Each treatment was thoroughly mixed and placed in the 120 mL containers which were then fully immersed in deionised water for 24 h to allow the superabsorbent to reach equilibrium. A control treatment without the superabsorbent was also prepared and underwent the same immersion treatment. Five replicates of each treatment were conducted. After 24 h, the containers were raised to drain the excess water until no further water was observed coming out of the bottom of the container and the weight was recorded. The containers were then placed without any covering into a temperature/humidity control cabinet (Thermoline L+M – 150-GD) kept at 23 °C and 70% relative humidity. Samples were weighed every day. Water retention was calculated as follows:

$$\text{Water retention (\%)} = \frac{\mathrm{m_i}}{\mathrm{m_o}} \text{ x } 100 \quad (2)$$

Where m_i refers to the mass of the sample at day i, and m_o is the mass of the control after being fully saturated with water (day 0).

During the first experiment, samples were allowed to dry without any further addition of water. This experiment concluded when no further mass loss was detected.

During the second experiment, samples were prepared and incubated under the same conditions as described previously, over a period of 28 days. In this case, further addition of deionised water was performed whenever the percentage of the water in the control

190 treatment had decreased to 10% or less. This typically required between 10 – 12 mL of
191 water at 8 – 10 day intervals. This same volume of water was added to all the other
192 treatments at that point.

193 **Table 2.** Application rate and mass of superabsorbent used in the experiment.

Application rate (%)	Mass of superabsorbent (g)	Mass of soil (g)
0.0	0.00	50.00
0.2	0.10	49.90
0.5	0.25	49.75
1.0	0.50	49.50

194

195 ## 2.4 Microbial activity studies

196 Soil incubation studies were performed with two types of superabsorbent: freeze-dried
197 and oven-dried at 50 °C. For each type, treatments were prepared by adding the
198 superabsorbent at the same application rates as mentioned in section 2.3 to prepare 50 g of
199 soil mixture. Deionised water was added to reach 60% WHC. Two different control
200 treatments were prepared: one without any superabsorbent and another with a basal
201 application of fertiliser and 1% wt of superabsorbent. The fertiliser was applied at an
202 equivalent rate of 60 kg ha^{-1} of N, 70 kg ha^{-1} of P and 60 kg ha^{-1} of K based on the soil
203 analysis. The fertiliser was thoroughly mixed with the soil. Five replicates were conducted
204 for each treatment. Samples were incubated at 23 °C and 80% relative humidity in a
205 temperature/humidity control cabinet (Thermoline L+M – 150-GD).

206 Gas samples were collected at days 1, 3, 5, 7, 14, 21 and 28 using the static chamber
207 method adapted from van Zwieten et al. (2010). Briefly, the containers containing the
208 incubated, treated soils were sealed and soil gas emissions were allowed to accumulate for
209 exactly 10 minutes (based on a CO_2 emission curve previously conducted). A gas tight
210 syringe (SGE Analytical Scientific) was used to extract an aliquot of soil gas emissions
211 through a chlorobutyl septum and was then introduced into a pre-evacuated Labco®
212 exetainer vial. Collected gases were analysed for CO_2 using an Agilent Technologies

7890A Gas Chromatography – Thermal Conductivity Detector (GC-TCD) and GC-Flame Ionization Detector (FID).

The flux rate, F_{CO2}, was calculated using equation 3 and noted as mg CO_2/m^2h:

$$F_{CO_2} = \frac{b \times V_{CH} \times MW_{CO_2} \times 60 \times 10^6}{A_{CH} \times MV_{corr} \times 10^9} \quad (3)$$

Where b is the CO_2 concentration measured in ppm/min, V_{CH} is the volume of the measuring chamber, MW_{CO_2} is the molecular weight of CO_2 (44 g/mol), A_{CH} refers to the basal area of the measuring chamber and MV_{corr} is the temperature corrected molecular weight volume calculated using equation 4:

$$MV_{corr} = 0.02241 \times \left(\frac{273.15+T}{273.15}\right) \quad (4)$$

Where T is the air temperature during the measurement and 0.02241 is the molar volume of an ideal gas at 273.15 K, 1 atm.

2.5 Biodegradation studies

Superabsorbent biodegradation was evaluated for two types of superabsorbent: freeze-dried and oven-dried at 50 °C. For each type, superabsorbent was added to soil at the application rates specified in section 2.3 to an overall total of 10 g. Deionised water was added to reach 60 % WHC. Similar to the microbial activity studies, two different control treatments were prepared: one without any superabsorbent and another with a basal rate of fertiliser and 1%wt of superabsorbent, as previously described. The latter was to review the effect of the fertiliser on superabsorbent biodegradation. Five replicates were conducted for each treatment. Samples were incubated at 23 °C and 80% relative humidity in a temperature/humidity control cabinet (Thermoline L+M – 150-GD). Samples were destructively sampled at days 1, 3, 5, 7, 14, 21 and 28, dried in an oven at 60 °C and stored frozen at -20 °C until required.

Biodegradation was measured using the acid digestion method adapted from Sluiter et al. (2008) to hydrolyse cellulose in the soil to glucose and glucuronic acid which were then measured. In brief, 3 mL of 72% sulphuric acid was added to 5 g of treated soil at room temperature. The mixture was placed in a water bath at 30 °C and incubated for 60 min.

During this time, the mixture was occasionally stirred every 5 to 10 minutes to ensure even acid – soil contact. Dilution to 4% sulphuric acid was made by adding 83 mL of deionised water followed by autoclaving for 60 minutes at 121 °C. After cooling to room temperature, the soil was removed by filtration and the supernatant retained and neutralised to pH 5 – 6 using calcium carbonate. When neutralisation was completed, the solids were separated by centrifugation at 4400 rpm for 10 min. The supernatant was collected and analysed through high performance liquid chromatography (HPLC) using a BioRad Amminex HPX-87H column, 0.005M sulphuric acid as the mobile phase, with a refractive index detector at a temperature of 40 °C and a flow rate of 0.4 mL/min.

2.6 Swelling studies

i) Soil water extract. Water was extracted from the soil according to the saturation extract method adapted from Sparks (1996). A mass of 1 kg of air-dried soil was weighed into a beaker. Deionised water was added to the soil until it was nearly saturated and the mixture was left at room temperature for 3 h to allow the dissolution of the soluble salts. More water was added while stirring, until the soil paste shined and a soil-water paste was formed. The soil paste was left at room temperature for another 2 h. The soil paste was then filtered under vacuum using a Buchner funnel and filter paper. The filtrate (i.e. soil water extract) was centrifuged at 4400 rpm for 10 min to further separate any remaining solids from the soil water extract.

The soil water extract was characterised by Environmental Analysis Laboratories, at Southern Cross University (Environmental Analysis Laboratory 2020), using Rayment and Lyons (Rayment 2011) standard methods (Table 3).

Table 3. Characteristics of the calcarosol soil water extract used in the experiments.

Parameter	Water extract
pH	6.80
Electrical conductivity (µS/m)	536.02
Aluminium (mg/L)	31.90
Iron (mg/L)	16.40

Silicon (mg/L)	63.90
Calcium (mg/L)	9.27
Magnesium (mg/L)	4.44
Potassium (mg/L)	8.39
Sodium (mg/L)	72.60
Chloride (mg/L)	39.90
Sulphur (mg/L)	28.90
Phosphorus (mg/L)	9.90

ii) Swelling capacity. The swelling capacity of the superabsorbents was measured in the soil water extracts obtained in previous section to simulate real environment conditions, with comparison to DI water. The swelling capacity and swelling rate were determined by weighing the samples before and after immersion in the soil water extract over different periods of time (1, 5, 15, 30, 60, 90, 150 and 250 minutes) at room temperature. The swelling capacity was calculated as follows:

$$\text{Swelling capacity, } Q = \frac{m_t - m_d}{m_d} \quad (5)$$

where m_t is the weight of the swollen gel at time t and m_d refers to the weight of the dried sample. Results are reported as the average and standard deviation of triplicates.

2.7 Data analysis

The microbial activity data was analysed statistically using a One-way ANOVA (analysis of variance) to evaluate differences between the means of the control and treatments. Dunnett's test was used to determine any significant differences between the control and the treatments. Biodegradation studies were analysed statistically using a t-test analysis to evaluate differences between the means the treatments. Both analyses were performed using GraphPad Prism 9.0.2.

3.0 RESULTS

3.1 Swelling

The swelling capacity of the three nanocellulose superabsorbents in soil water extracts is expressed as a function of time (Figure 1). All superabsorbents show a similar behaviour. Swelling uptake reaches a plateau after an initial absorption rate. In all cases, superabsorbents required up to 150 minutes to reach maximum capacity. Freeze-dried superabsorbent is characterised by an initial rapid swelling with most of it occurring during the first minutes. In contrast, superabsorbents dried via evaporation show a slower swelling rate.

Swelling at equilibrium is dictated by the drying technique used to prepare the superabsorbent and the swelling media employed (Figure 2). While SAP oven-dried at 50 °C achieves the highest absorption capacity in deionised water, freeze-dried SAP has the highest swelling capacity in soil water extracts of 90 g water/g superabsorbent. This is followed by SAP oven-dried at 50 °C and at 105 °C being 55 and 40 g water/g superabsorbent, respectively.

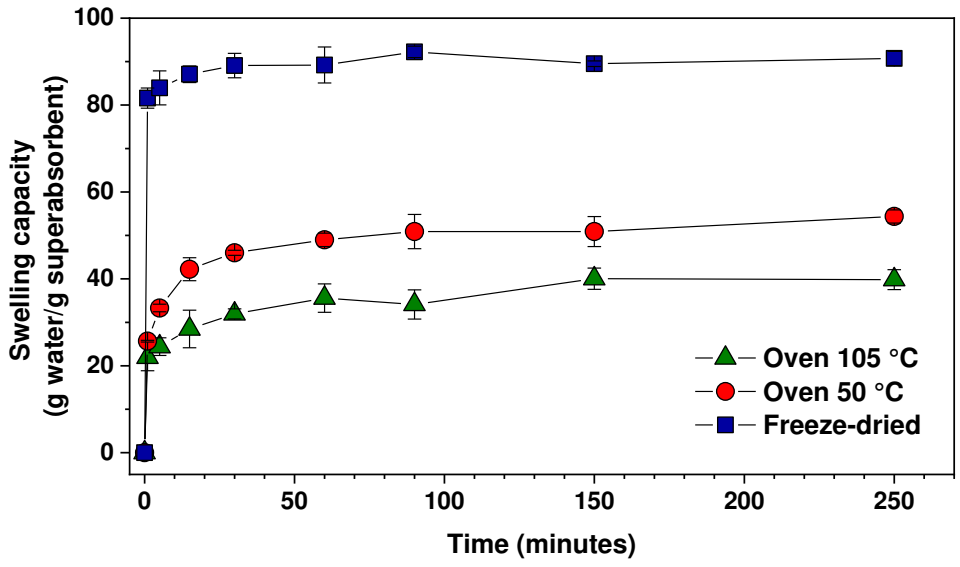

Figure 1. Effect of the drying process on the swelling capacity of nanocellulose superabsorbents immersed in soil water as a function of time. Results are reported as mean ± standard deviation (n=3).

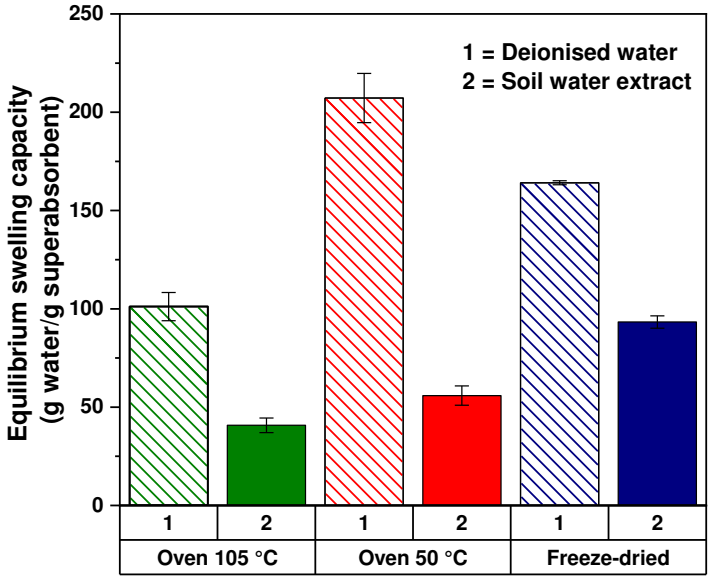

298

299 **Figure 2.** Effect of the drying process on the swelling capacity of nanocellulose superabsorbents at
300 equilibrium. Comparison of deionized water with soil water extract. Results are reported as mean
301 +/- standard deviation (n=3)

302 ## 3.2 Soil water retention

303 The water retention of the soil amended with the nanocellulose superabsorbents was
304 evaluated under two conditions: with and without further addition of water after the initial
305 irrigation – day 0 (Figure 3a-f). In all treatments, soil water retention increases as the
306 nanocellulose SAP application rate increases. This is independent of the superabsorbent
307 type. Soil amended with freeze-dried SAP shows the maximum water retention of 2.3 times
308 higher than soils without superabsorbent (control) (Figure 3a). While controls required
309 approximately 10 days to reach constant weight, soils amended with 1 wt% application rate
310 of any superabsorbent took between 25 to 33 days, 2.3 to 3 times longer time compared to
311 the control.

312 For all treatments, the water retention effectiveness decreases with increasing number of
313 irrigation cycles. This is noted via two different indicators. Firstly, the water retention of
314 the soil treated with any superabsorbent decreases with increasing irrigation cycles. For
315 example, the water retention of the soil treated with 1.0 wt% oven-dried at 50 °C SAP
316 changes from 170% in the first cycle to 110% and 85% in the second and third irrigation
317 cycles, respectively. Secondly, the difference between the water retention of the soil

treatments and the control decreases as the irrigation number increases. Both indicators suggest a decrease in the superabsorbent efficiency.

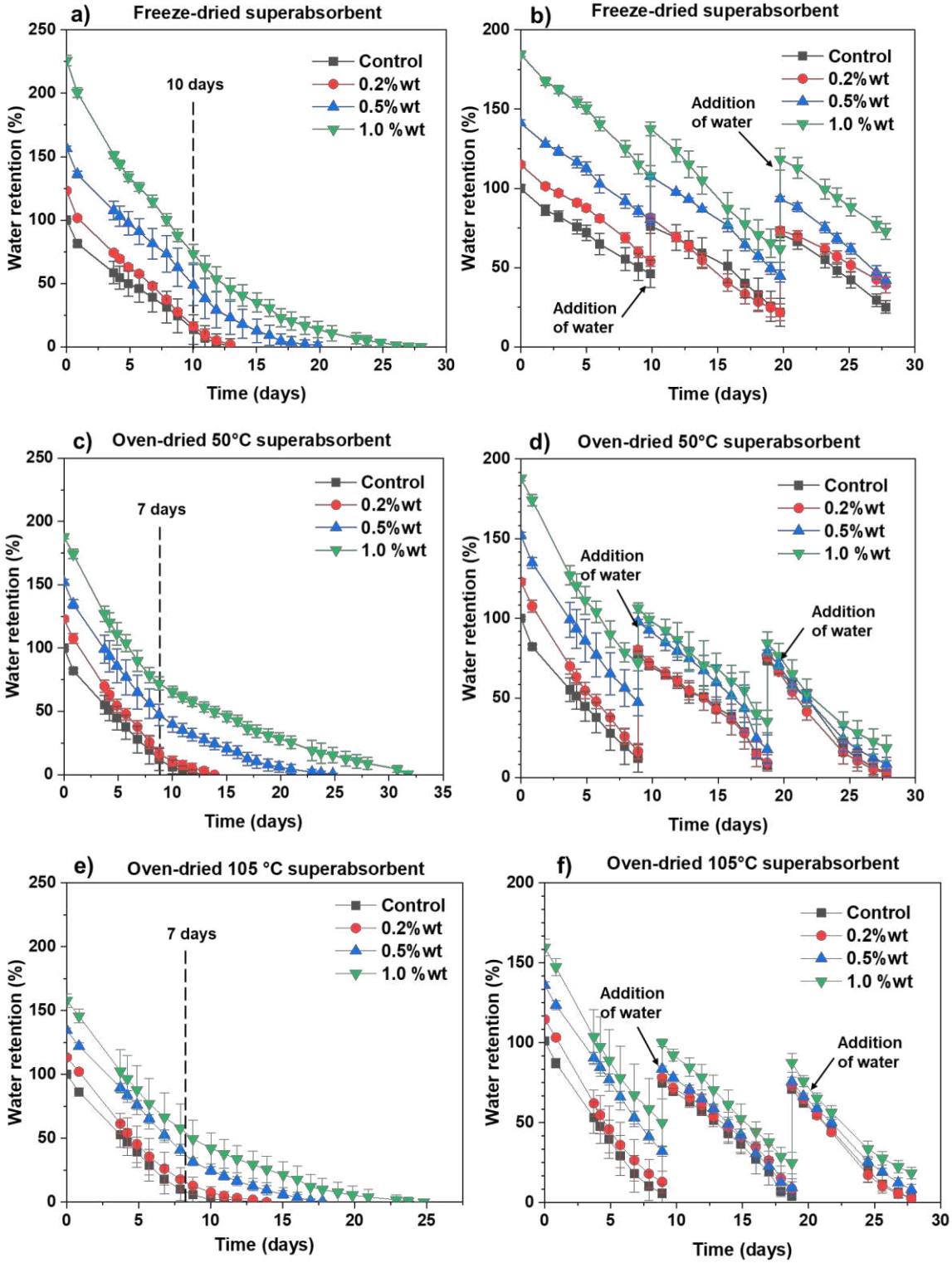

Figure 3. Water retention of soil treated with different nanocellulose superabsorbents over a period of 28 days with and without further addition of water after initial irrigation: (a and b) freeze-dried SAP, (c and d) oven-dried 50 °C SAP and (e and f) oven-dried 105 °C SAP. Results are reported as mean ± standard deviation (n=5).

3.3 Microbial activity

In general, for both types of superabsorbent, CO_2 emissions (i.e. respiration rates) increase with time and application rate (Figure 4). This increase is more statistically significant when freeze-dried superabsorbent is used, as noted by Dunnett's test. The difference between the control and soil treated with 1 %wt SAP ranges between 900 mg CO_2/m^2h to 1800 mg CO_2/m^2h for 50 °C oven-dried and freeze-dried SAP, respectively. These respiration rates signify the response of the soil microbial community to the presence of this nanocellulose superabsorbent. Similarly, fertilised soil amended with 1 %wt of any SAP exhibits an increase of CO_2 emissions compared to the soil treatments without fertiliser.

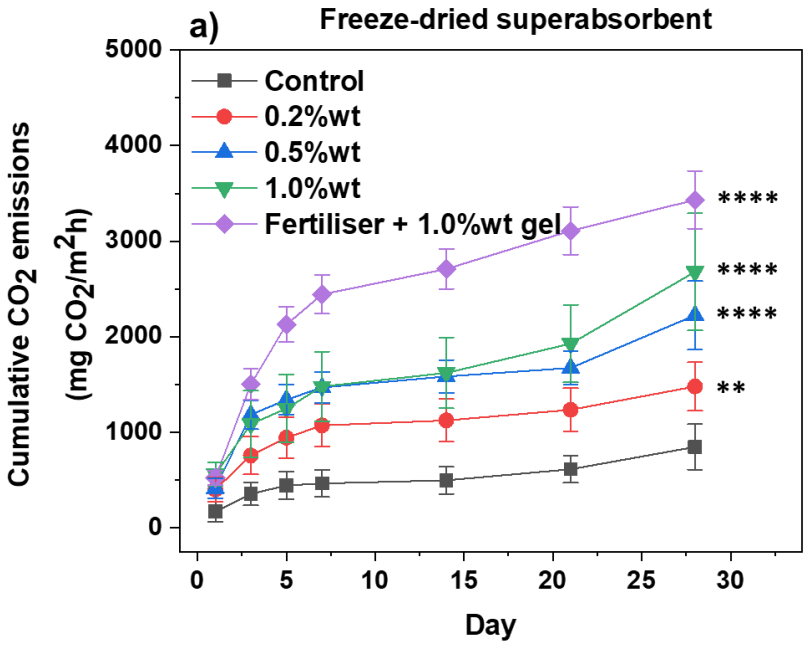

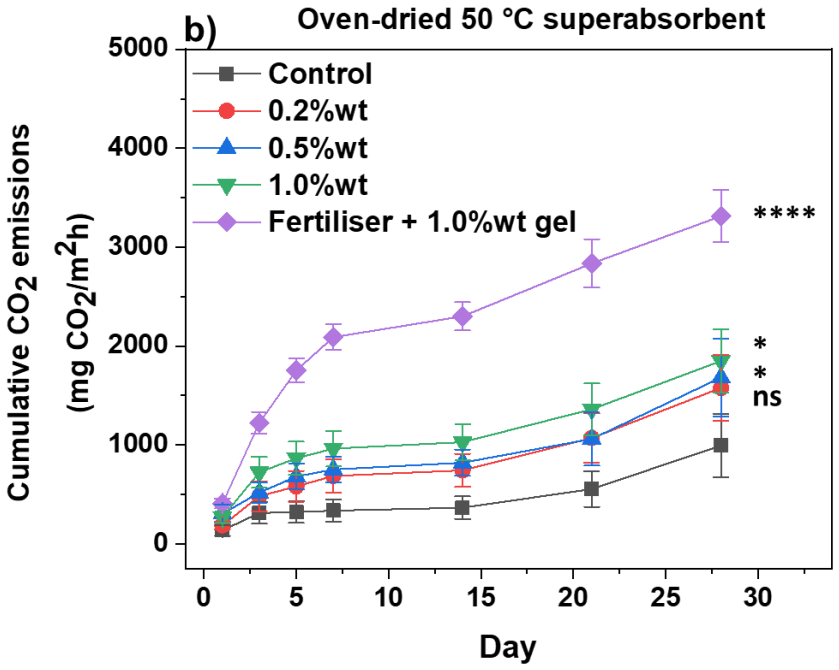

338

339 **Figure 4.** Cumulative CO_2 emissions of soil treated with different application rates of (a) freeze-
340 dried superabsorbent and (b) oven-dried 50 °C superabsorbent. Results are reported as mean ±
341 standard deviation (n=5). Statistical difference according to One-way ANOVA analysis followed by
342 Dunnett's test against control is indicated. Here, ns = no significant difference, * represents $p \leq 0.05$,
343 ** denotes $p \leq 0.01$ and **** is $p \leq 0.0001$.

344 ## 3.4 Biodegradation

345 For the soil used in this study, the rate of biodegradation is dependent upon the type and
346 application rate of superabsorbent (Figure 5). For soil treated with 0.2 wt% superabsorbent,
347 both freeze-dried and oven-dried SAP follow the same degradation trend and
348 approximately 40% of the initial SAP remains after 28 days exposure. No statistical
349 difference is observed between soil treatments with either 0.2 wt% or 0.5 wt% application
350 rate of superabsorbent. However, a difference in the biodegradation rate and SAP type is
351 observed when the application rate increases. For the 1 wt% treatment, freeze-dried SAP
352 degradation starts after 7 days exposure, whereas degradation of oven-dried SAP
353 throughout the 28 days of exposure is slow and almost negligible. Fertiliser addition to 1
354 wt% treatment significantly increases the degradation rate; both nanocellulose
355 superabsorbents exhibit similar rates compared to 0.2 wt% treatment.

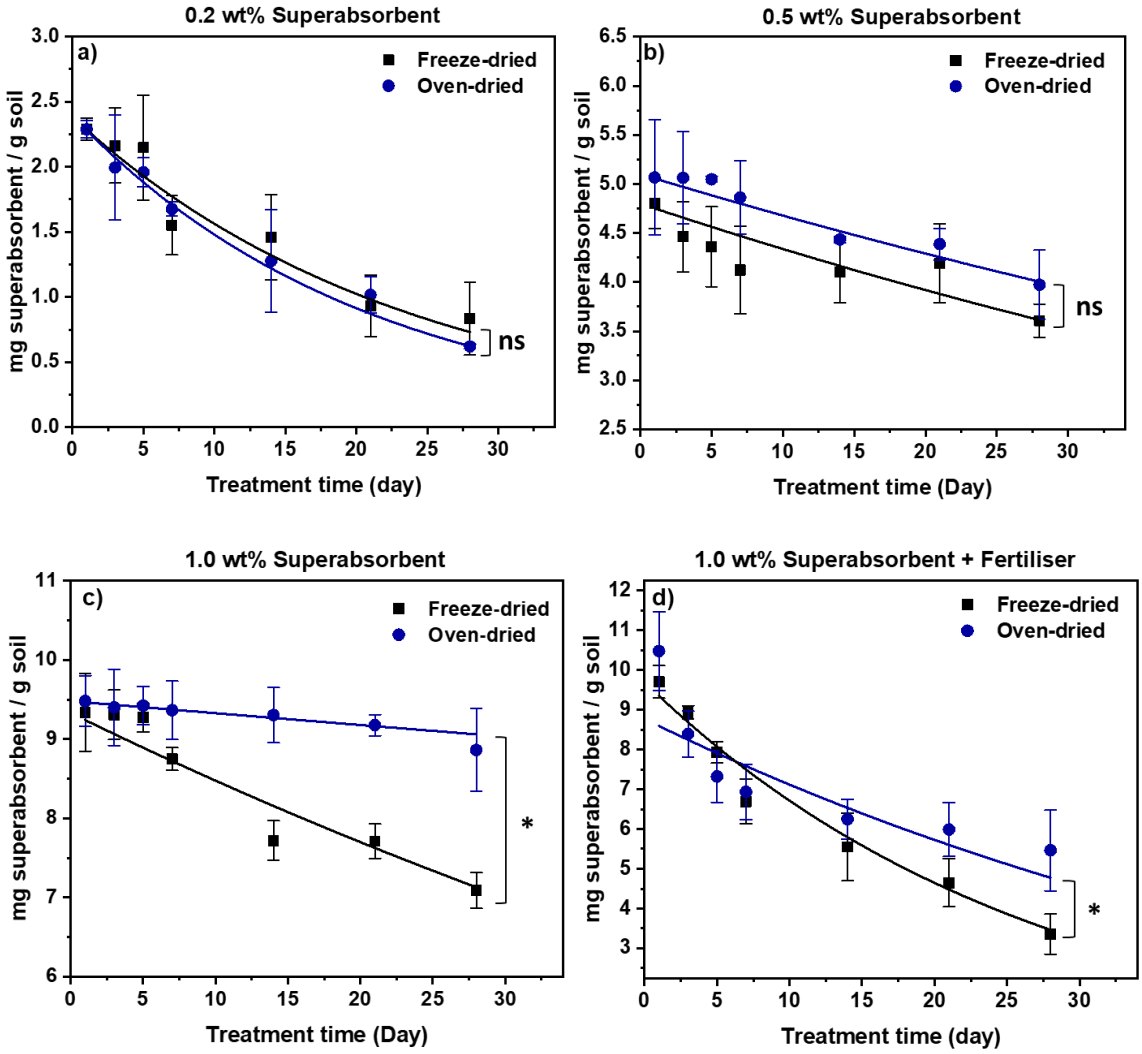

Figure 5. Effect of drying process on the superabsorbent biodegradation overtime in soil. (a) 0.2 wt%, (b) 0.5 wt%, (c) 1 wt% and (d) 1 wt% superabsorbent application rate + fertiliser addition. Results are reported as mean ± standard deviation (n=5). Statistical difference according to unpaired t-test. Here, ns= no significant difference between treatments, * is $p \leq 0.05$.

4.0 DISCUSSION

4.1 Effect of ionic strength on superabsorbent performance

The swelling capacity of nanocellulose-based superabsorbent was measured in the soil-water to evaluate their performance. A decrease in the absorption capacity of the superabsorbent results when salt concentration increases, independent of its type. This is because the swelling ability is driven by the difference in osmotic pressure inside and outside the polymer network caused by the movement of the counterions in the system (Mendoza et al. 2019). These osmotic effects are diminished with increasing concentrations

of salt, resulting in a decrease in swelling (Mondal 2019). To measure the sensitivity of the superabsorbent materials towards the soil water extracts, the ionic sensitivity (IS) was measured as follows (Kabiri et al. 2005):

$$\mathrm{IS\ (f)} = 1 - \frac{Q_s}{Q_d} \qquad (6)$$

Where Q_s refers to the swelling in salt solution and Q_d is the swelling in deionised water. Superabsorbents with lower f values are preferred for their performance, as higher f values mean a higher absorbency loss of the superabsorbent in salt solutions (Mondal 2019).

The ionic sensitivity (f) value of the superabsorbents studied is displayed in Figure 6. Oven-dried 50 °C SAP shows a higher ionic sensitivity compared to the others. This is attributed to its morphology, characterised by a high pore area and large number of small pores in the nanometre scale (Barajas-Ledesma et al. 2020). This increases the number of accessible COO^- groups in the superabsorbent network, whereas the swelling mechanism of freeze-dried SAP is mainly driven by physical entrapment of water. A higher number of accessible COO- groups indicates a higher cation charge, which in the presence of salt solutions, results in a higher salt sensitivity and absorbency loss for oven-dried 50 °C superabsorbents.

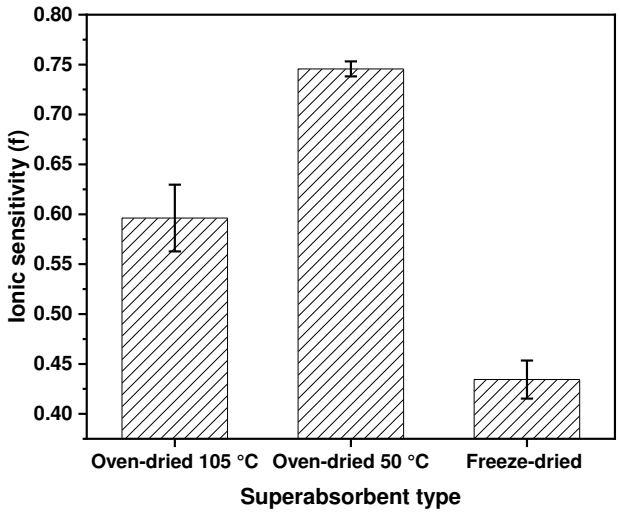

Figure 6. Ionic sensitivity value of the superabsorbents treated with soil water extracts. A low f value indicates a lower drop of swelling capacity when salt solution replace water. Results are reported as mean ± standard deviation (n=3).

4.2 Effect of application rate on soil water retention

Addition of nanocellulose superabsorbent increases the water retention of the soil tested. Soil amended with freeze-dried superabsorbent achieved the highest water retention, at all application rates, followed by 50 °C oven-dried and 105 °C oven-dried SAP. These results are directly related to the SAP porous structure (Barajas-Ledesma et al. 2020). Such an increase in water content is hypothesised to increase the period of water available for the plant, as measured from the soils water evaporation rates. The evaporation rates of the soils amended with the highest superabsorbent application (1.0 wt%) were slower than those of the controls. This results in a delay of the permanent wilting point by up to 20 days, reducing the water requirement of plants (Akhter J et al. 2004; Demitri et al. 2013). This also confirms that nanocellulose derived SAP can retain water in soils for significantly longer periods. (Cannazza et al. 2014).

There are three different drying regimes for each type of superabsorbent and application rate. The first corresponds to the water evaporating from the soil. This regime starts from day 0 up to day 8-10 for freeze-dried and oven-dried SAPs. This is followed by a transitionary phase, as the soil is completely dried and the superabsorbent starts to release water. Finally, the last drying regime corresponds to the evaporation of water from the superabsorbent itself. This regime is indicated by the different slopes of each SAP depending on the application rate and lasts from the transitionary phase onwards. These regimes can be used to correlate the soil moisture and superabsorbent efficiency over time.

Interestingly, soil treated with 1.0 wt% of freeze-dried SAP loses water at a faster rate than oven-dried 50 °C SAP. This difference in drying rate is attributed to their difference in SAP structure and the influence of soil structure and how it interacts with the SAP. Freeze-dried superabsorbent is a foamy-like material characterised by an open structure, whereas oven-dried SAP is a thin-film with pores ranging in the nanometre scale (Barajas-Ledesma et al. 2020). When the freeze-dried nanocellulose SAP dries, its structure collapses, leaving large pores in the soil which increase soil matrix porosity and facilitate water evaporation (Beven and Germann 1982).

Comparing water retention of the soil treatments after several irrigation cycles, all treatments presented a similar behaviour: high-water absorption in the first cycle which decreased in the subsequent cycles. This was independent of the application rate. This decrease is mainly attributed to two factors. Firstly, the metal ions in the soil that are released in the presence of water. When the superabsorbent absorbs this water, these ions strongly bind to the carboxylate groups of the nanocellulose, blocking their active negative sites and decreasing absorbency. SAP blockage increases with each further cycle of irrigation and drying (Shahid et al. 2012). This effect was reported previously by Spagnol et al. (2012), who found an increase formation of crosslinking points due to the physical interaction of multivalent cations (e.g. Mg^{2+} and Ca^{2+}) and the carboxylate groups present in superabsorbents based on poly(acrylamide-co-acrylate) and cellulose nanowhiskers. The second main factor affecting the SAP efficiency is its degradation (Cannazza et al. 2014).

4.3 Superabsorbent effect on microbial community and its biodegradation

Respiration rates of the soil amended with nanocellulose SAP increased with increasing application rate. This is because the addition of a carbon source to the soil increases the population of carbon decomposing microbes which results in an increase in respiration rate (Schlesinger and Andrews 2000; Högberg and Ekblad 1996; Gallardo and Schlesinger 1994; Fontaine et al. 2004). Adding fertiliser further accelerates soil respiration rates for both types of superabsorbent. This is because of the increase in microbial biomass by nutrient addition which boosts the decomposition rate of soil carbon (Gallardo and Schlesinger 1994).

Respiration rates of each treatment are related to the superabsorbent degradation rate in soil which follows the negative exponential function (Hartmann and Appel 2006):

$$C(t) = C_0 e^{-kt} \quad (7)$$

Where C(t) stands for the superabsorbent concentration (mg/g) in the soil at time t of incubation, C_0 is the superabsorbent concentration at day 0, and k is the rate constant of the superabsorbent decay with time (day^{-1}). The decay rate constants, k, for all the treatments

are listed in Table 4. Decay rate constants varied widely from 0.001 d^{-1} to 0.048 d^{-1} depending on the SAP type and application rate. This model successfully described decomposition rates of carbon sources such as cellulose or manure (Cabassi et al. 2008; Chmolowska et al. 2017; Hadas et al. 2004). The decay rate constant of the soil amended with 0.2 wt% SAP was similar for nanocellulose freeze-dried and oven-dried 50 °C, ranging between 0.042 and 0.048 d^{-1}, respectively. The rate of superabsorbent decomposition in soil is independent of the type of superabsorbent (either freeze-dried or oven-dried). Considering that the SAP is composed of more than 90% cellobiose units with the remainder being oxidised glucose units, its decomposition rate can be compared to that of cellulose, reported to range from 0.03 and 0.06 d^{-1}(Hartmann and Appel 2006; Hadas et al. 2004). The calculated values of soil amended with 0.2 wt% SAP correspond to this range. The rate of superabsorbent breakdown is affected by soils and incubation conditions: moisture content and temperature.

This rate is also governed by the initial population of microbes and nutrients available in soil. For example, decomposition of 0.5 wt% oven-dried SAP in soil is delayed until day 5. This is due to the time required to build up the microbial biomass in soil necessary to kick off the decomposition process. Such effect is not observed in soil amended with freeze-dried SAP because of its porous structure which increases soil porosity. This increases oxygen diffusion and air permeability (Domżał et al. 1991), which facilitates the increase in microbial biomass. However, a delay in degradation is observed as the application rate increases. This is most likely due to nutrient depletion impacting the microbial population. This is supported by the fertiliser addition to 1 wt% soil treatments which accelerates SAP breakdown, exhibiting similar rates to 0.2 wt% SAP in soil without fertiliser.

Table 4. Decay rate constants of freeze-dried and oven-dried superabsorbents. Results are reported as mean ± standard deviation (n=5).

Cellulose application rate (wt%)	Cellulose initial concentration (mg/g)	Decay rate constant (day^{-1})	R^2
Freeze-dried			

0.2 wt%	2.28 ± 0.08	0.042 ± 0.0038	0.97
0.5 wt%	4.80 ± 0.25	0.010 ± 0.0006	0.90
1.0 wt%	9.33 ± 0.48	0.009 ± 0.0007	0.91
1.0 wt% + Fertiliser	9.70 ± 0.41	0.037 ± 0.0022	0.97
Oven-dried 50 °C			
0.2 wt%	2.28 ± 0.06	0.048 ± 0.0007	0.99
0.5 wt%	5.06 ± 0.58	0.008 ± 0.0009	0.81
1.0 wt%	9.48 ± 0.32	0.001 ± 0.0001	0.91
1.0 wt% + Fertiliser	10.47 ± 0.99	0.017 ± 0.0052	0.74

5.0 CONCLUSION

Carboxylated nanocellulose superabsorbent polymers (SAP) were evaluated as water retentor for agricultural use. SAPs were made from TEMPO mediated oxidation of cellulose followed by high pressure homogenisation and drying. Three drying methods were studied: freeze-dried and oven-dried at low (50 °C) and high (105°C) temperatures. The effect of the nanocellulose superabsorbents on the water retention and microbial community in a calcarosol soil was analysed and the swelling capacity on soil water and biodegradation rate were determined.

The water retention of soil increases with application rate of superabsorbent. The extent of this increase in water holding capacity and the profile of water retention over time are dependent on the type of SAP. These water retention properties decrease as the superabsorbent degrades. Soil amended with freeze-dried superabsorbent has the highest water retention, followed by 50 °C oven-dried and 105 °C oven-dried SAP. The high ionic sensitivity of 50 °C oven-dried SAP is due to its high pore area and numerous accessible COO- groups. Soil amended with this superabsorbent remains moist the longest. This increase in water content prolongs the period of water available for the plant, delaying the permanent wilting point by up to 20 days.

Soil respiration rate increases as a function of superabsorbent application rate. This is related to the SAP decomposition rate which, in the calcarosol soil used in this study, mainly occurs within 30 days exposure, independently of the type of nanocellulose superabsorbent. This decomposition rate is governed by the nutrient availability and the initial microbial biomass in the soil. Carboxylated nanocellulose-based superabsorbents are attractive alternatives to replace our current non-biodegradable and unsustainable petroleum SAP for agricultural use. The full characterisation of plant growth, including crop productivity and soil sustainability as well as refinements of the SAP structural alteration required to prolong its biodegradability are now needed.

6.0 DECLARATIONS

Funding. financial support through the grant IH130100016.

Conflicts of interest. The authors declare they have no financial interests.

Availability of data material. All authors declare that all data and materials support their published claims and comply with field standards.

Authors contribution. All authors contributed to the preparation of the manuscript. The final version of the manuscript was approved by all authors.

Code availability. Not applicable

Ethics approval. Not applicable

Consent to participate. All authors give consent to participate

Consent for publication. All authors give consent for publication

7.0 REFERENCES

Abrisham ES, Jafari M, Tavili A, Rabii A, Zare Chahoki MA, Zare S, et al. (2018). Effects of a super absorbent polymer on soil properties and plant growth for use in land reclamation. Arid land research and management, 32(4), 407-420. doi:https://doi.org/10.1080/15324982.2018.1506526.

Ahmed EM (2015). Hydrogel: Preparation, characterization, and applications: A review. Journal of Advanced Research, 6(2), 105-121. doi:https://doi.org/10.1016/j.jare.2013.07.006.

Akhter J, Mahmood K, Malik KA, Mardan A, Ahmad M, MM I (2004). Effects of hydrogel amendment on water storage of sandy loam and loam soils and seedling growth of barley, wheat and chickpea. Plant, Soil and Environment, 50(10), 463-469.

Azeem B, KuShaari K, Man ZB, Basit A, Thanh TH (2014). Review on materials & methods to produce controlled release coated urea fertilizer. Journal of Controlled Release, 181, 11-21. doi:https://doi.org/10.1016/j.jconrel.2014.02.020.

523 Barajas-Ledesma RM, Patti AF, Wong VNL, Raghuwanshi VS, Garnier G (2020). Engineering
524 nanocellulose superabsorbent structure by controlling the drying rate. Colloids and Surfaces A:
525 Physicochemical and Engineering Aspects, 600. doi:10.1016/j.colsurfa.2020.124943.

526 Bashari A, Rouhani Shirvan A, Shakeri M (2018). Cellulose-based hydrogels for personal care
527 products. Polymers for Advanced Technologies, 29(12), 2853-2867. doi:10.1002/pat.4290.

528 Beven K, Germann P (1982). Macropores and water flow in soils. Water Resources Research, 18(5),
529 1311-1325. doi:10.1029/WR018i005p01311.

530 Cabassi G, Gallina PM, Barzaghi S, Cattaneo TMP, Bechini L (2008). Near Infrared Monitoring of
531 Mineralisation of Liquid Dairy Manure in Agricultural Soils. Journal of Near Infrared Spectroscopy,
532 16(1), 59-69. doi:10.1255/jnirs.762.

533 Cannazza G, Cataldo A, De Benedetto E, Demitri C, Madaghiele M, Sannino A (2014).
534 Experimental Assessment of the Use of a Novel Superabsorbent polymer (SAP) for the Optimization
535 ofWater Consumption in Agricultural Irrigation Process. Water, 6(7), 2056-2069.
536 doi:10.3390/w6072056.

537 Chen P, Zhang WA, Luo W, Fang Ye (2004). Synthesis of superabsorbent polymers by irradiation
538 and their applications in agriculture. Journal of Applied Polymer Science, 93(4), 1748-1755.
539 doi:10.1002/app.20612.

540 Chmolowska D, Hamda N, Laskowski R (2017). Cellulose decomposed faster in fallow soil than in
541 meadow soil due to a shorter lag time. Journal of Soils and Sediments, 17(2), 299-305.
542 doi:10.1007/s11368-016-1536-9.

543 Curvello R, Raghuwanshi VS, Garnier G (2019). Engineering nanocellulose hydrogels for
544 biomedical applications. Advances in Colloid and Interface Science, 267, 47-61.
545 doi:https://doi.org/10.1016/j.cis.2019.03.002.

546 Demitri C, Scalera F, Madaghiele M, Sannino A, Maffezzoli A (2013). Potential of Cellulose-Based
547 Superabsorbent Hydrogels as Water Reservoir in Agriculture. International Journal of Polymer
548 Science, 2013. doi:http://dx.doi.org/10.1155/2013/435073.

549 Department of Agriculture WatE, (2020). Water for food. Australian Government.
550 https://www.agriculture.gov.au/water/water-for-food. Accessed 12/06/2020 2020.

551 Domżał H, Gliński J, Lipiec J (1991). Soil compaction research in Poland. Soil and Tillage Research,
552 19(2), 99-109. doi:https://doi.org/10.1016/0167-1987(91)90079-D.

553 Environmental Analysis Laboratory SCU, (2020). Agricultural soil testing.
554 https://www.scu.edu.au/environmental-analysis-laboratory---eal/analytical-services/agricultural-
555 soil-testing/. Accessed 31/07/2020 2020.

556 Fontaine S, Bardoux G, Benest D, Verdier B et al. (2004). Mechanisms of the Priming Effect in a
557 Savannah Soil Amended with Cellulose. Soil Science Society of America Journal, 68(1), 125-131.

558 Gallardo A,Schlesinger WH (1994). Factors limiting microbial biomass in the mineral soil and forest
559 floor of a warm-temperate forest. Soil Biology and Biochemistry, 26(10), 1409-1415.
560 doi:https://doi.org/10.1016/0038-0717(94)90225-9.

561 Ghorbani S, Eyni H, Bazaz SR, Nazari H, Asl LS, Zaferani H, et al. (2019). Hydrogels Based on
562 Cellulose and its Derivatives: Applications, Synthesis, and Characteristics. Polymer Science, Series
563 A, 60(6), 707-722. doi:10.1134/s0965545x18060044.

564 Gross JR (1990). The Evolution of Absorbent Materials. In L. Brannon-Peppas, & R. S. Harland
565 (Eds.), Studies in Polymer Science (pp. 3-22). Elsevier. doi:https://doi.org/10.1016/B978-0-444-
566 88654-5.50006-6.

567 Guilherme MR, Aouada FA, Fajardo AR, Martins AF, Paulino AT, Davi MFT, et al. (2015).
568 Superabsorbent hydrogels based on polysaccharides for application in agriculture as soil conditioner

569 and nutrient carrier: A review. European Polymer Journal, 72, 365-385.
570 doi:10.1016/j.eurpolymj.2015.04.017.

571 Guilherme MR, Reis AV, Paulino AT, Moia TA, Mattoso LHC, Tambourgi EB (2010). Pectin-based
572 polymer hydrogel as a carrier for release of agricultural nutrients and removal of heavy metals from
573 wastewater. Journal of Applied Polymer Science, n/a-n/a. doi:10.1002/app.32123.

574 Hadas A, Kautsky L, Goek M, Erman Kara E (2004). Rates of decomposition of plant residues and
575 available nitrogen in soil, related to residue composition through simulation of carbon and nitrogen
576 turnover. Soil Biology and Biochemistry, 36(2), 255-266.
577 doi:https://doi.org/10.1016/j.soilbio.2003.09.012.

578 Hartmann HP, Appel T (2006). Calibration of near infrared spectra for measuring decomposing
579 cellulose and green manure in soils. Soil Biology and Biochemistry, 38(5), 887-897.
580 doi:https://doi.org/10.1016/j.soilbio.2005.08.005.

581 Högberg P, Ekblad A (1996). Substrate-induced respiration measured in situ in a C3-plant ecosystem
582 using additions of C4-sucrose. Soil Biology and Biochemistry, 28(9), 1131-1138.
583 doi:https://doi.org/10.1016/0038-0717(96)00124-1.

584 Horton AA, Walton A, Spurgeon DJ, Lahive E, Svendsen C (2017). Microplastics in freshwater and
585 terrestrial environments: Evaluating the current understanding to identify the knowledge gaps and
586 future research priorities. Science of The Total Environment, 586, 127-141.
587 doi:https://doi.org/10.1016/j.scitotenv.2017.01.190.

588 Isbell RF. (2016). The Australian soil classification. Clayton South, VIC, Australia : CSIRO
589 Publishing.

590 Isogai A, Saito T, Fukuzumi H (2011). TEMPO-oxidized cellulose nanofibers
591 (10.1039/C0NR00583E). Nanoscale, 3(1), 71-85. doi:10.1039/C0NR00583E.

592 Kabir SMF, Sikdar PP, Haque B, Bhuiyan MAR, Ali A, Islam MN (2018). Cellulose-based hydrogel
593 materials: chemistry, properties and their prospective applications. Prog Biomater, 7(3), 153-174.
594 doi:10.1007/s40204-018-0095-0.

595 Kabiri K, Faraji-Dana S, Zohuriaan-Mehr MJ (2005). Novel sulfobetaine-sulfonic acid-contained
596 superswelling hydrogels. Polymers for Advanced Technologies, 16(9), 659-666.
597 doi:10.1002/pat.637.

598 Lavoine N, Bergström L (2017). Nanocellulose-based foams and aerogels: processing, properties,
599 and applications. Journal of Materials Chemistry A, 5(31), 16105-16117. doi:10.1039/c7ta02807e.

600 Li Q, McGinnis S, Sydnor C, Wong A, Renneckar S (2013). Nanocellulose Life Cycle Assessment.
601 ACS Sustainable Chemistry & Engineering, 1(8), 919-928. doi:10.1021/sc4000225.

602 Li S,Chen G (2020). Agricultural waste-derived superabsorbent hydrogels: Preparation,
603 performance, and socioeconomic impacts. Journal of Cleaner Production, 251, 119669.
604 doi:https://doi.org/10.1016/j.jclepro.2019.119669.

605 Liliana Serna C, Guancha-Chalapud MA (2017). Natural fibers for hydrogels production and their
606 applications in agriculture. Acta Agronómica, 66(4), 495-505.
607 doi:http://dx.doi.org/10.15446/acag.v66n4.56875.

608 Mendoza L, Hossain L, Downey E, Scales C, Batchelor W, Garnier G (2019). Carboxylated
609 nanocellulose foams as superabsorbents. J Colloid Interface Sci, 538, 433-439.
610 doi:10.1016/j.jcis.2018.11.112.

611 Mondal IH. (2019). Cellulose-Based Superabsorbent Hydrogels. Saharanpur, India:

612 Montesano FF, Parente A, Santamaria P, Sannino A, Serio F (2015). Biodegradable Superabsorbent
613 Hydrogel IncreasesWater Retention Properties of Growing Media and Plant Growth. Agriculture
614 and Agricultural Science Procedia, 4, 451-458. doi:10.1016/j.aaspro.2015.03.052.

615 Müller C. BA, Popp A., Waha K., Fader M., (2010) Climate change impacts on agricultural yields
616 P. I. f. C. I. Research *World Development Report* Germany: Potsdam Institute for Climate Impact
617 Research.

618 Organisation for Economic Co-operation and Development Managing water sustainably is key to
619 the future of food and agriculture. https://www.oecd.org/agriculture/topics/water-and-agriculture/.
620 Accessed 12/06/2020 2020.

621 Ramos L, Berenstein G, Hughes EA, Zalts A, Montserrat JM (2015). Polyethylene film
622 incorporation into the horticultural soil of small periurban production units in Argentina. Science of
623 The Total Environment, 523, 74-81. doi:https://doi.org/10.1016/j.scitotenv.2015.03.142.

624 Rayment GE. (2011). Soil chemical methods Australasia. Collingwood, Vic.: Collingwood, Vic. :
625 CSIRO Pub.

626 Reddy Kathi S. (2019) Effect of different doses of superabsorbent polymer (SAP) on water and
627 nitrogen retention in soil, and on the growth and development of tomato and determination of
628 optimal rate of SAP. College of Graduate Studies Texas A&M University-Kingsville

629 Schlesinger WH, Andrews JA (2000). Soil respiration and the global carbon cycle. Biogeochemistry,
630 48(1), 7-20. doi:http://dx.doi.org/10.1023/A:1006247623877.

631 Shahid SA, Qidwai AA, Anwar F, Ullah I, Rashid U (2012). Improvement in the Water Retention
632 Characteristics of Sandy Loam Soil Using a Newly Synthesized Poly(acrylamide-co-acrylic
633 Acid)/AlZnFe2O4 Superabsorbent Hydrogel Nanocomposite Material. Molecules, 17(8), 9397-
634 9412. doi:http://dx.doi.org/10.3390/molecules17089397.

635 Shen X, Shamshina JL, Berton P, Gurau G, Rogers RD (2016). Hydrogels based on cellulose and
636 chitin: fabrication, properties, and applications (10.1039/C5GC02396C). Green Chemistry, 18(1),
637 53-75. doi:10.1039/C5GC02396C.

638 Shewan HM, Stokes JR (2013). Review of techniques to manufacture micro-hydrogel particles for
639 the food industry and their applications. Journal of Food Engineering, 119(4), 781-792.
640 doi:https://doi.org/10.1016/j.jfoodeng.2013.06.046.

641 Sluiter A, Hames B, Ruiz R, Scarlata C, Sluiter J, Templeton D, et al. (2008). Determination of
642 structural carbohydrates and lignin in biomass, in: Laboratory Analytical Procedure (LAP). National
643 Renewable Energy Laboratory.

644 Spagnol C, Rodrigues FHA, Neto AGVC, Pereira AGB, Fajardo AR, Radovanovic E, et al. (2012).
645 Nanocomposites based on poly(acrylamide-co-acrylate) and cellulose nanowhiskers. European
646 Polymer Journal, 48(3), 454-463. doi:10.1016/j.eurpolymj.2011.12.005.

647 Sparks DLe. (1996). Methods of soil analysis. Part 3, Chemical methods. Madison, Wisconsin: Soil
648 Science Society of America: American Society of Agronomy.

649 Steinmetz Z, Wollmann C, Schaefer M, Buchmann C, David J, Tröger J, et al. (2016). Plastic
650 mulching in agriculture. Trading short-term agronomic benefits for long-term soil degradation?
651 Science of The Total Environment, 550, 690-705.
652 doi:https://doi.org/10.1016/j.scitotenv.2016.01.153.

653 van Zwieten L, Kimber S, Morris S, Downie A, Berger E, Rust J, et al. (2010). Influence of biochars
654 on flux of N2O and CO2 from Ferrosol (Article). Australian Journal of Soil Research, 48, 555+.
655 https://link.gale.com/apps/doc/A241179274/AONE?u=monash&sid=AONE&xid=088435d9.

656 Varanasi S, He R, Batchelor W (2013). Estimation of cellulose nanofibre aspect ratio from
657 measurements of fibre suspension gel point. Cellulose, 20(4), 1885-1896. doi:10.1007/s10570-013-
658 9972-9.

659 Zhang H, Yang M, Luan Q, Tang H, Huang F, Xiang X, et al. (2017). Cellulose Anionic Hydrogels
660 Based on Cellulose Nanofibers As Natural Stimulants for Seed Germination and Seedling Growth.
661 J Agric Food Chem, 65(19), 3785-3791. doi:10.1021/acs.jafc.6b05815.

662 Zhou Y, Fu S, Zhang L, Zhan H (2013). Superabsorbent nanocomposite hydrogels made of
663 carboxylated cellulose nanofibrils and CMC-g-p(AA-co-AM). Carbohydrate Polymers, 97(2), 429-
664 435. doi:https://doi.org/10.1016/j.carbpol.2013.04.088.

665 Zohuriaan-Mehr MJ, Kabiri, Kourosh. (2008). Superabsorbent Polymer Materials: A review. Iranian
666 Polymer Journal, 17(6), 451-477.

667 Zohuriaan-Mehr MJ, Omidian H, Doroudiani S, Kabiri K (2010). Advances in non-hygienic
668 applications of superabsorbent hydrogel materials (journal article). Journal of Materials Science,
669 45(21), 5711-5735. doi:10.1007/s10853-010-4780-1.

670

Figures

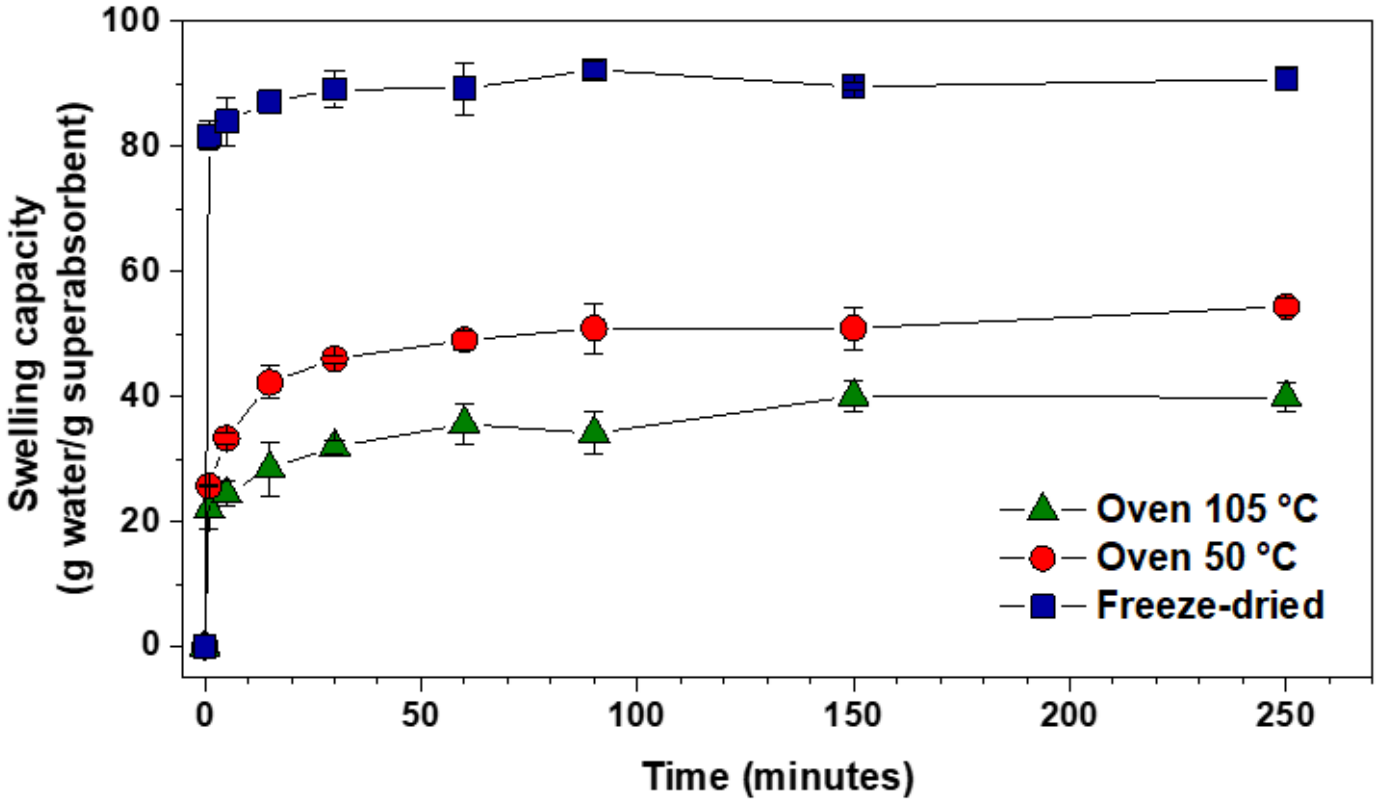

Figure 1

Effect of the drying process on the swelling capacity of nanocellulose superabsorbents immersed in soil water as a function of time. Results are reported as mean ± standard deviation (n=3).

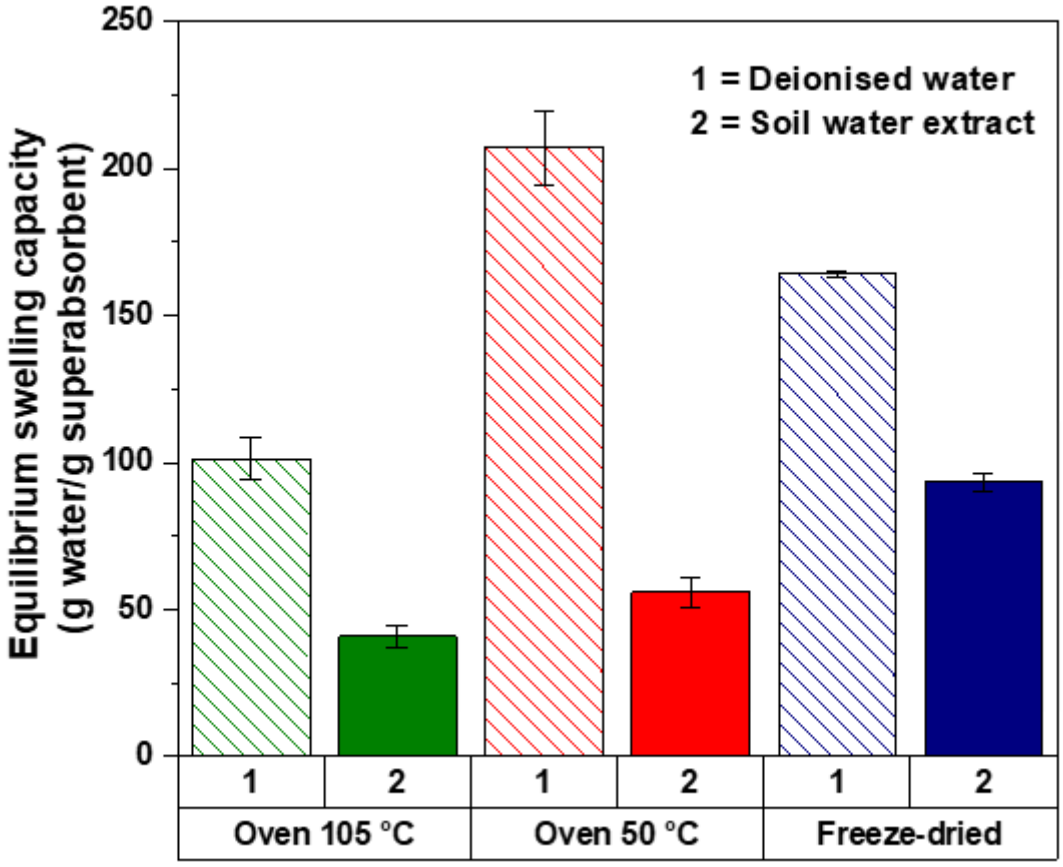

Figure 2

Effect of the drying process on the swelling capacity of nanocellulose superabsorbents at equilibrium. Comparison of deionized water with soil water extract. Results are reported as mean +/- standard deviation (n=3)

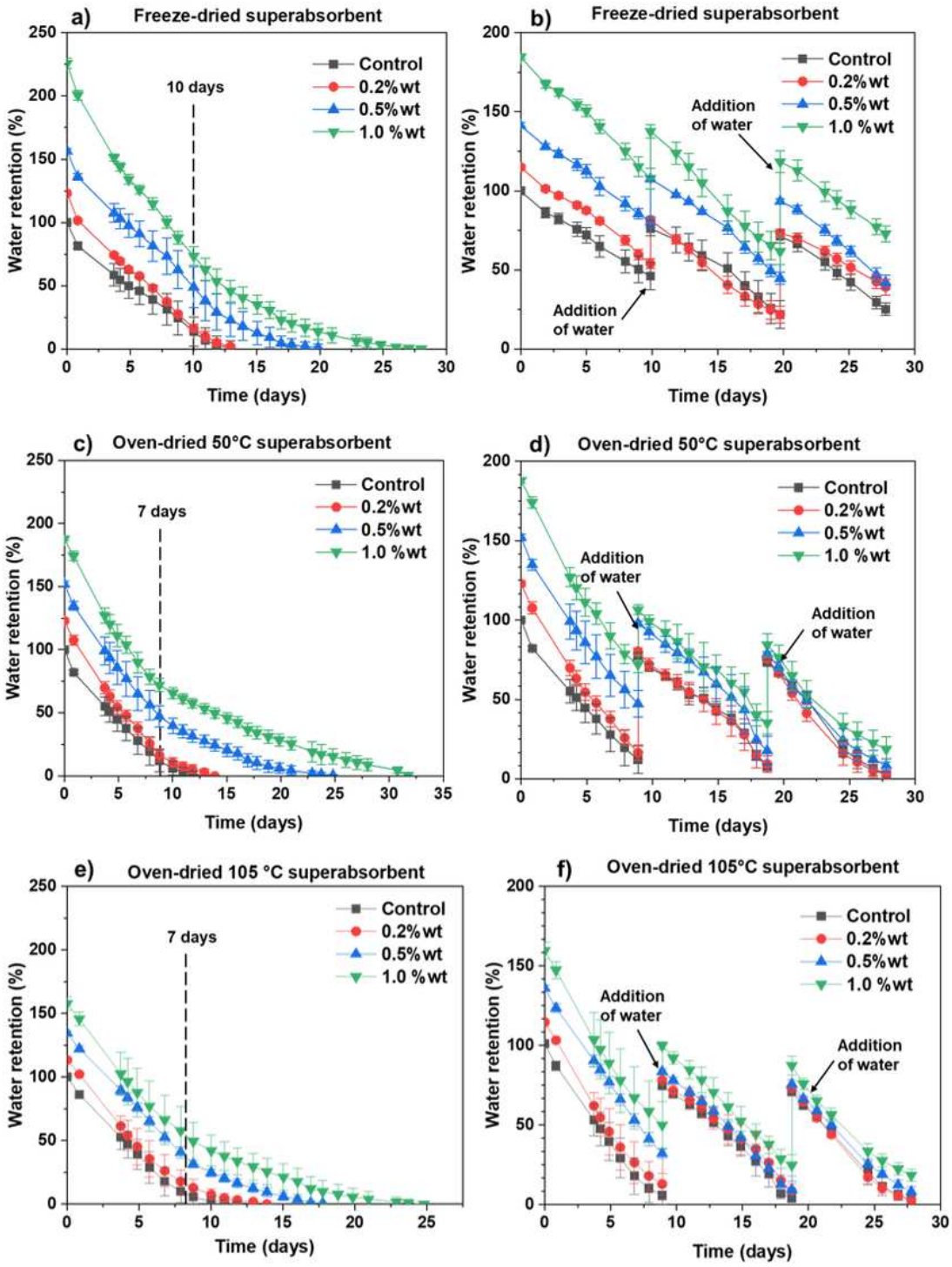

Figure 3

Water retention of soil treated with different nanocellulose superabsorbents over a period of 28 days with and without further addition of water after initial irrigation: (a and b) freeze-dried SAP, (c and d) oven-dried 50 °C SAP and (e and f) oven-dried 105 °C SAP. Results are reported as mean ± standard deviation (n=5).

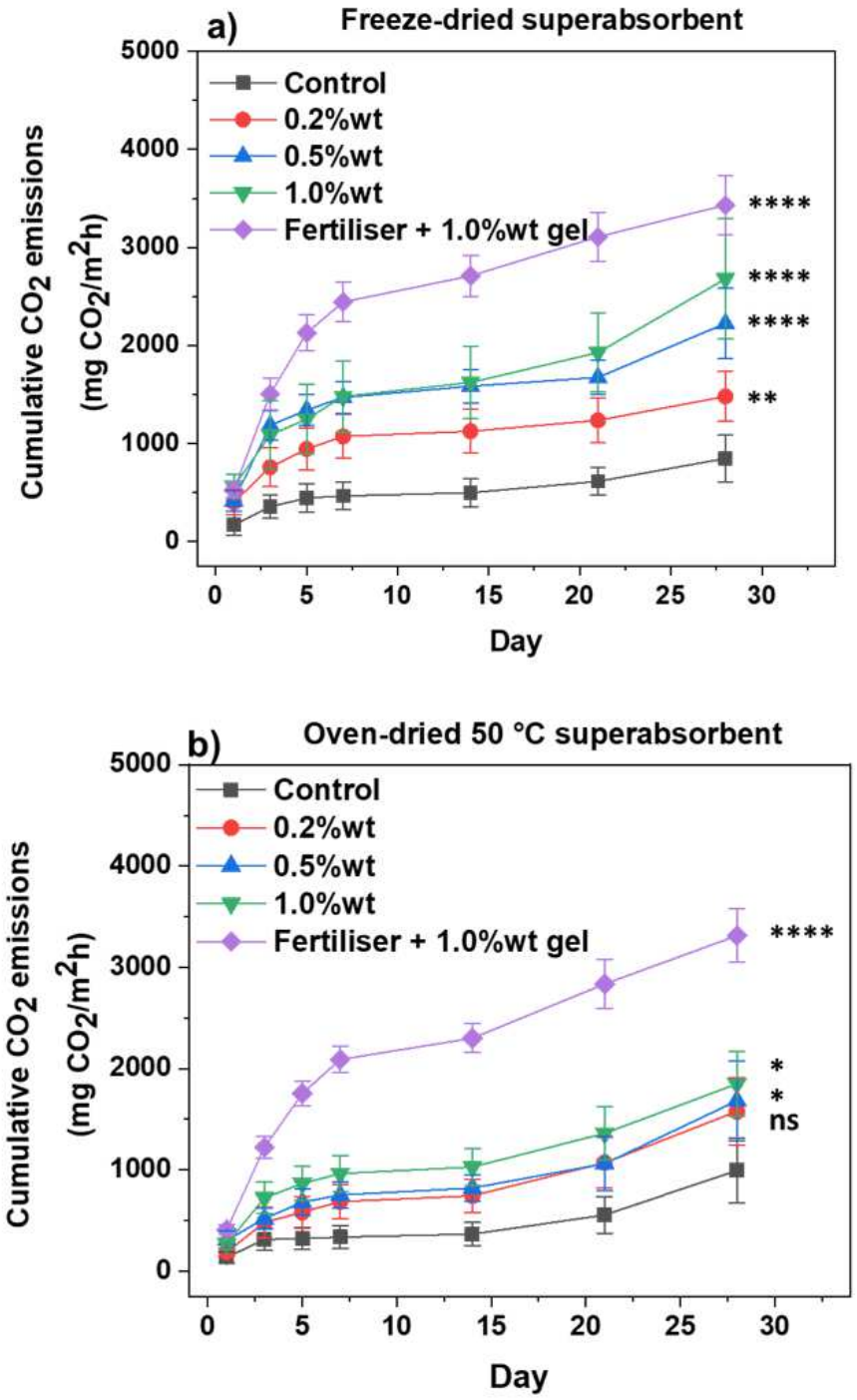

Figure 4

Cumulative CO2 emissions of soil treated with different application rates of (a) freeze-dried superabsorbent and (b) oven-dried 50 °C superabsorbent. Results are reported as mean ± standard deviation (n=5). Statistical difference according to One-way ANOVA analysis followed by Dunnett's test against control is indicated. Here, ns = no significant difference, * represents $p \leq 0.05$, ** denotes $p \leq 0.01$ and **** is $p \leq 0.0001$.

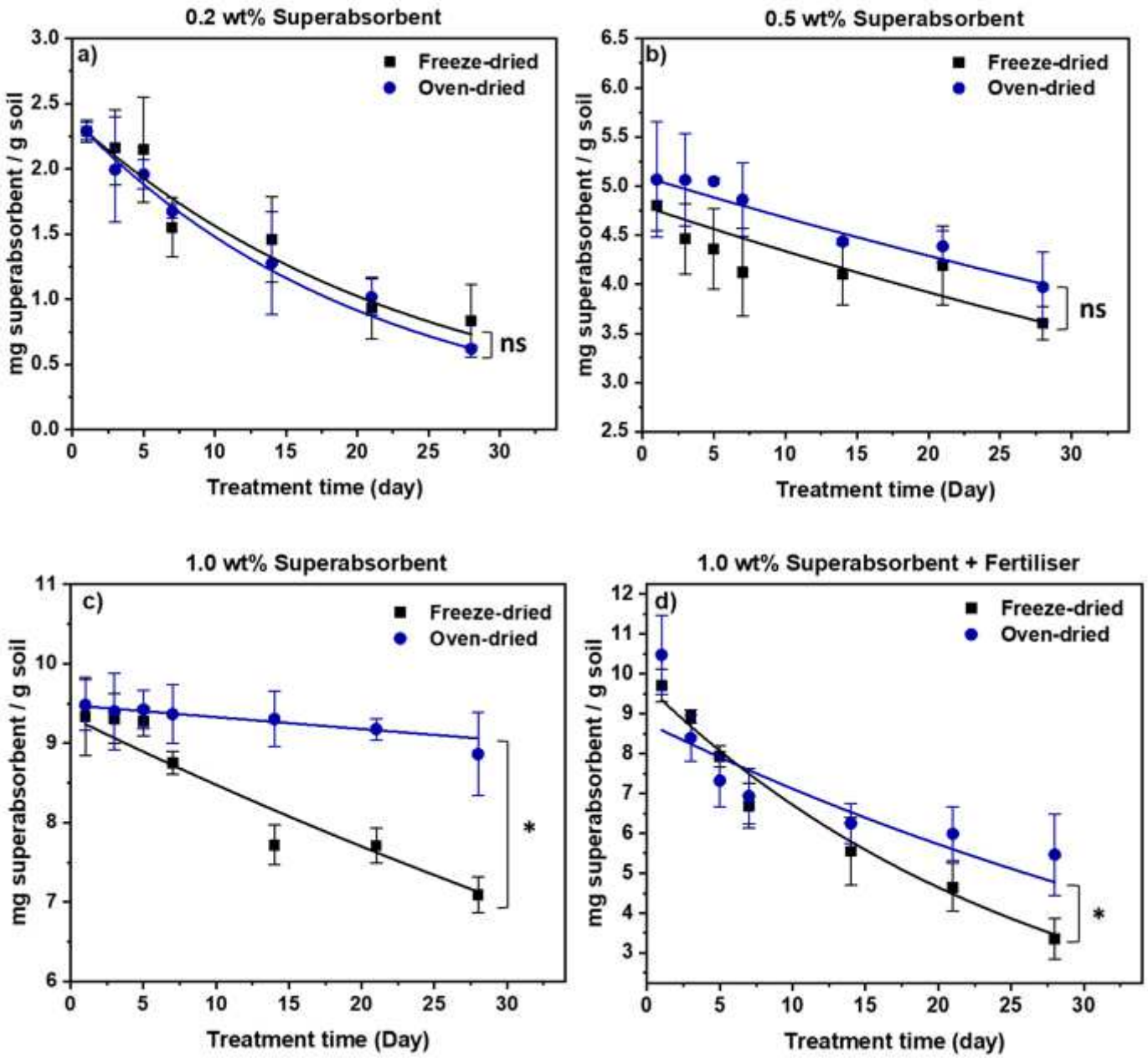

Figure 5

Effect of drying process on the superabsorbent biodegradation overtime in soil. (a) 0.2 wt%, (b) 0.5 wt%, (c) 1 wt% and (d) 1 wt% superabsorbent application rate + fertiliser addition. Results are reported as mean ± standard deviation (n=5). Statistical difference according to unpaired t-test. Here, ns= no significant difference between treatments, * is $p \leq 0.05$.

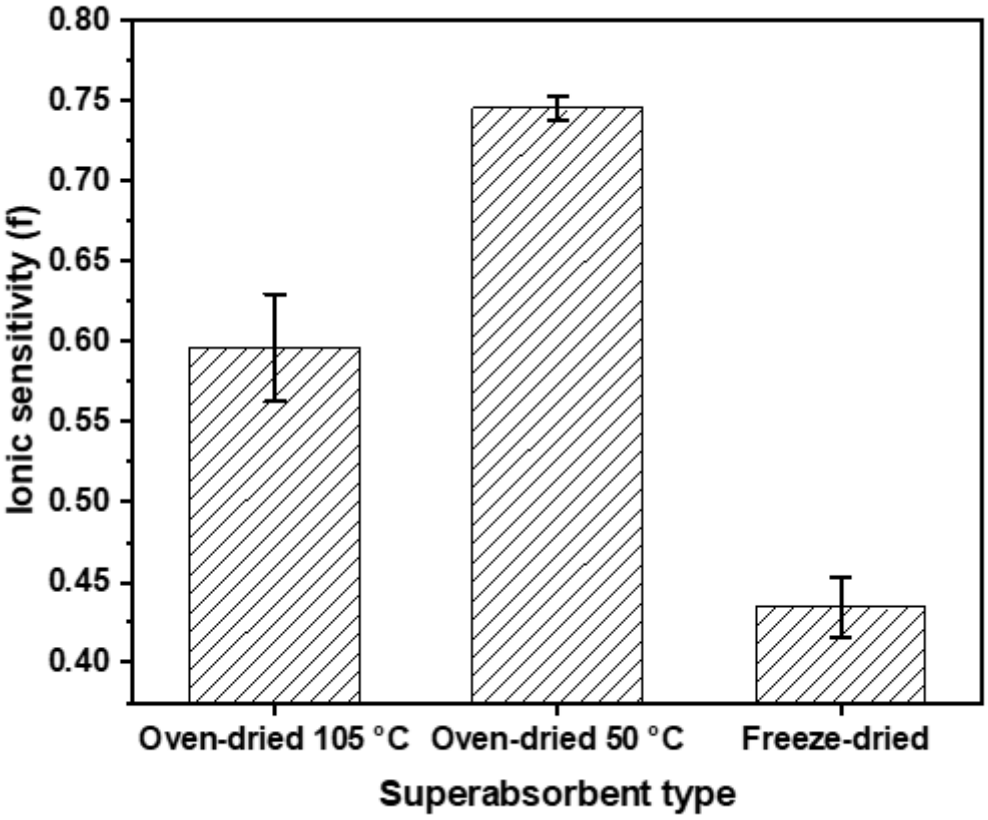

Figure 6

Ionic sensitivity value of the superabsorbents treated with soil water extracts. A low f value indicates a lower drop of swelling capacity when salt solution replace water. Results are reported as mean ± standard deviation (n=3).

Supplementary Files

This is a list of supplementary files associated with this preprint. Click to download.

- Graphicalabstract.tif